





# Flexible silver nanowire transparent conductive films prepared by an electrostatic adsorption self-assembly process

Boda Zheng<sup>1,2</sup> , Qingsheng Zhu<sup>1,2,\*</sup> , and Yang Zhao<sup>1,2</sup> 

<sup>1</sup>Shenyang National Laboratory for Materials Science, Institute of Metal Research, Chinese Academy of Sciences, Shenyang 110016, China

<sup>2</sup>School of Materials Science and Engineering, University of Science and Technology of China, Shenyang 110016, China

Received: 21 July 2018

Accepted: 4 December 2018

Published online:  
14 December 2018

© Springer Science+Business  
Media, LLC, part of Springer  
Nature 2018

## ABSTRACT

In this work, we reported a facile approach to fabricate silver nanowire (AgNW) networks on flexible substrates. Through immersing the modified poly (ethylene terephthalate) with positively charged functional group into the AgNW dispersion with anionic dispersant, a flexible AgNW transparent conductive film was formed by electrostatic adsorption self-assembly process. Even without a post-treatment process, the as-prepared flexible AgNW films exhibited excellent optoelectrical property, low surface roughness and high reliability. It was shown that the insulating dispersant on AgNWs could be effectively removed by an ion bombardment method and then greatly decreased the sheet resistance of AgNW networks. Because of the nature of spontaneous adsorption, this preparation method can be suitable for an arbitrary shaped substrate, which will broaden the application of AgNW conductive films in optoelectronic devices.

## Introduction

Transparent conductive films (TCFs) are essential components for many optoelectronic devices such as solar cells, liquid crystal displays, organic light emitting diodes and touch panels [1–4]. Due to the increasing need for wearable optoelectronic devices, the flexible and stretchable TCFs have been intensively studied [5]. Tin-doped indium oxide (ITO) has been widely used in commercial TCFs. However, due to indium resources scarcity, high process cost, high deposition temperature, and especially its intrinsic

brittleness, the usage of ITO will be seriously limited in emerging flexible optoelectronic devices [6]. Currently, there is an urgent need to develop the next-generation flexible TCFs. Many potential alternatives including graphene [7, 8], carbon nanotubes [9, 10], metal or metal nanowires [11–14] and hybrids of these [3, 15] have been paid high attention. Among of them, silver nanowires (AgNWs) possessing excellent optical and electrical properties, high mechanical robustness, good flexibility and comparatively high chemical stability are considered as one of the most promising candidates [6, 14, 16, 17]. In the past

Address correspondence to E-mail: qszhu@imr.ac.cn

decade, a variety of methods had been presented to construct AgNW conductive films. The Meyer rod coating technique reported by Hu et al. [14] enabled scalable roll-to-roll deposition of AgNWs on a substrate. Selzer et al. [18] investigated a spray-coating process of AgNW conductive films. A dry transfer technique for transferring AgNW networks onto a flexible substrate was reported by Madaria et al. [19]. However, the above-mentioned methods encounter a difficulty that the films are only deposited on flat substrates with regular shape, which seriously limits the application of TCFs. In addition, without the usage of an organic binder or the mechanical pressure process, the prepared conductive films by these methods will usually suffer from poor adhesion between nanowires and flexible substrates. However, the binder can greatly increase the sheet resistance and the pressure treatment process can bring a risk of damaging weak flexible substrates.

The electrostatic adsorption method was early developed by Decher and others for the construction of ultrathin multilayer films of organic compounds [20–25]. Based on electrostatic adsorption principle, we proposed a novel preparation process of AgNW conductive films on flexible substrates. It was intended to produce an ultrathin film on the substrate through simply dipping a positively charged substrate into AgNW dispersion containing anion dispersant. This method is characterized by several significant advantages over the common methods. Firstly, the adhesion between substrates and AgNWs can be greatly enhanced by strong electrostatic adsorption [21]. Furthermore, since the process is based on spontaneous adsorption in solution, the AgNW networks can be formed on an arbitrary shaped substrate. For example, this process can coat AgNWs onto a cylindrical electrode, but the traditional methods cannot finish it. Therefore, this easily operated method is expected to expand the application of conductive films. The test results showed that the as-fabricated conductive films by this process possessed excellent optoelectrical performance, low surface roughness and high reliability.

It is known that the originally prepared AgNW films without a post-treatment may have a considerable sheet resistance ( $R_s$ ), which will restrict its immediate application. This large sheet resistance is mainly resulted from both the contact resistance between the NWs–NWs and the insulating ligands on the nanowires. For reducing the contact resistance, a

large number of post-treatment processes such as thermal or mechanical pressing, flash-induced plasmonic welding and integration with other materials have been developed [14, 26–28]. However, up to date, it is still a difficulty to remove the insulating ligands on the nanowires after forming AgNW films. In this work, we tried to use an ion bombardment method to remove the non-conductive dispersant on the AgNWs. It was found that the sheet resistance could be reduced to a large extent after the AgNW film was cleaned by this method.

## Experimental

### Fabrication of AgNW dispersion

A mixture of 0.8 g of polyvinylpyrrolidone (PVP) (MW: 58000) and 31.2 g of 1,2-propylene glycol (PG) was heated to 125 °C and stirred for 15 min in a reaction vessel. Then, 1.1 g of tetrabutylammonium chloride (TBAC) solution, 1.0 g of catechol solution and 10.7 g of silver nitrate ( $\text{AgNO}_3$ ) solution were added to the stirring mixture. After 140 min, 21.5 g  $\text{AgNO}_3$  solution was dripped into the reaction vessel drop by drop over a period of 330 min. The obtained solution was cooled down to room temperature. The resulting solution was diluted with methanol and centrifuged three times at 8000 rpm for 10 min to remove PG, PVP and other impurities in the supernatant. Then, the precipitate of AgNWs and Zonyl<sup>®</sup> FSP (Dupont, China) were added into a vessel with a certain amount of deionized water, and the concentration of AgNW dispersion was controlled in 0.5–3 mg mL<sup>-1</sup>. In addition, the weight ratio of the anionic dispersant and AgNWs was about 1:(10–30).

### Graft polymerization onto poly (ethylene terephthalate) (PET) film

A mixture of 1.95 g of *N, N'*-(dimethylamino) ethyl methacrylate (DMAEMA), 3.12 g of 1-bromododecane ( $\text{R}_{12}\text{Br}$ ) and 50 mL acetone was stirred for 5 h at 40 °C and quaternary amine monomer (DMAEMA- $\text{R}_{12}\text{Br}$ ) was successfully synthesized. A clean PET film was placed in a beaker containing 5 g DMAEMA- $\text{R}_{12}\text{Br}$ , 0.01 g of meta-sodium periodate ( $\text{NaIO}_4$ ) and 50 mL deionized water. Using ultraviolet (UV) radiation produced from a 1000 W high-pressure

mercury lamp (Ergu Photoelectric Corporation, Shenzhen, China) irradiated the film at 40 °C for 3 h.

### Ion bombardment treatment process

To reduce sheet resistance of the conductive film, ion bombardment produced by a precision ion etching system (RES 101, Leica, Germany) was used to remove non-conductive polymers of its surface. In addition, the system voltage and current were controlled in 1–2 kV and 0.5–1 mA, respectively.

### Characterization

X-ray photoelectron spectrometer (XPS) (ESCALAB 250, Thermofisher VG, America) and Acid Orange 7 (98%, Aladdin Industrial Corporation, China) were used to detect the graft polymerization of DMAEMA- $R_{12}Br$  onto PET films. The pristine AgNWs and redispersed AgNWs were characterized using Fourier transform infrared spectroscopy (FTIR) (NICOLET 6700, Thermo Scientific, America) and XPS. Zeta potentials were measured by a ZS Zetasizer apparatus (Malvern Zetasizer Nano-ZS90, UK) and a solid surface zeta potential analyzer (SURPASS, Antor Paar, Austria). The morphologies of TCFs were characterized by scanning electron microscopy (SEM) (SUPRA 55 Sapphire, Zeiss, Germany) and the surface roughness was observed using an atomic force microscopy (AFM) (INNOVA, Bruker, Germany) with a tapping mode. The optical transmittance ( $T$ ) was measured using a UV-NIR spectrophotometer (CARY 5000, Agilent, China), in which a bare substrate was used as a blank sample to acquire the transmittance data. The measurement of the sheet resistance was carried out on a 4-point probes resistivity measurement system (RTS-9, China). The cyclic bending test was performed using a custom-designed apparatus.

## Results and discussion

The preparation process of the AgNW conductive film on PET substrate is schematically illustrated in Fig. 1a. Firstly, the graft polymerization of the PET film was achieved in aqueous solution with a reagent of quaternary amine monomers under the condition of UV radiation [29]. After graft polymerization, the modified PET film would be positively charged in

solution. The as-prepared AgNWs were carefully cleaned and then dispersed in aqueous solution with an anionic surface-active agent of Zonyl® FSP. After ultrasonic and stirring processes, a stable AgNW dispersion could be obtained when the negatively charged molecules adsorbed on AgNWs. Then the modified PET film was dipped into the AgNW dispersion. By strong electrostatic adsorption, the AgNWs were deposited and formed a uniform network on the PET substrate. In this self-assembly process by electrostatic adsorption, the AgNW network density could be easily controlled by adjusting the amount of graft polymerization and the concentration of AgNW dispersion. A moderate density of AgNW networks could generate the optimum combination of sheet resistance and optical transmittance. On the other hand, it was worth noted that this film preparation process by spontaneous adsorption was not limited regarding the size and shape of substrates. Figure 1b shows the molecular structures of the applied anionic surfactant of Zonyl® FSP and cationic surfactant of DMAEMA- $R_{12}Br$ .

In XPS analysis, the high-resolution spectra of C 1s, O 1s, N 1s and Br 3d regions of the virgin PET film and the modified PET film are shown in Fig. 2. The O 1s, N 1s and Br 3d intensities were normalized concerning the C 1s intensity. As shown in Fig. 2a, the C 1s spectrum of the virgin PET film could be divided into three peaks by curve fitting. The binding energies in three peaks were 284.6 eV, 286.2 eV and 288.6 eV, respectively, and it was known that the virgin film possessed three types of carbon functional groups, i.e., benzene ring, C–C–O and O–C=O. Based on the area ratio of carbon peaks, the ratio of carbon atoms in three functional groups was calculated to be 61:22:17, being nearly identical with the theoretical value of 60:20:20 [30]. The XPS O 1s core level spectrum of the virgin PET film contained two types of oxygen functional groups. They could be recognized as C–O (533.0 eV) and C=O (531.4 eV) by binding energy. The ratio of oxygen atoms in two functional groups was also consistent with the theoretical value [30]. Nevertheless, it was noted that there were no obvious peaks in the N 1s and Br 3d spectra of the virgin PET film. For the modified PET film, there were two new peaks in the C 1s spectrum compared with the virgin PET film, as shown in Fig. 2b. According to the binding energies of new peaks, it was determined that the corresponding functional groups were C–C (284.8 eV) and C–N (285.8 eV),

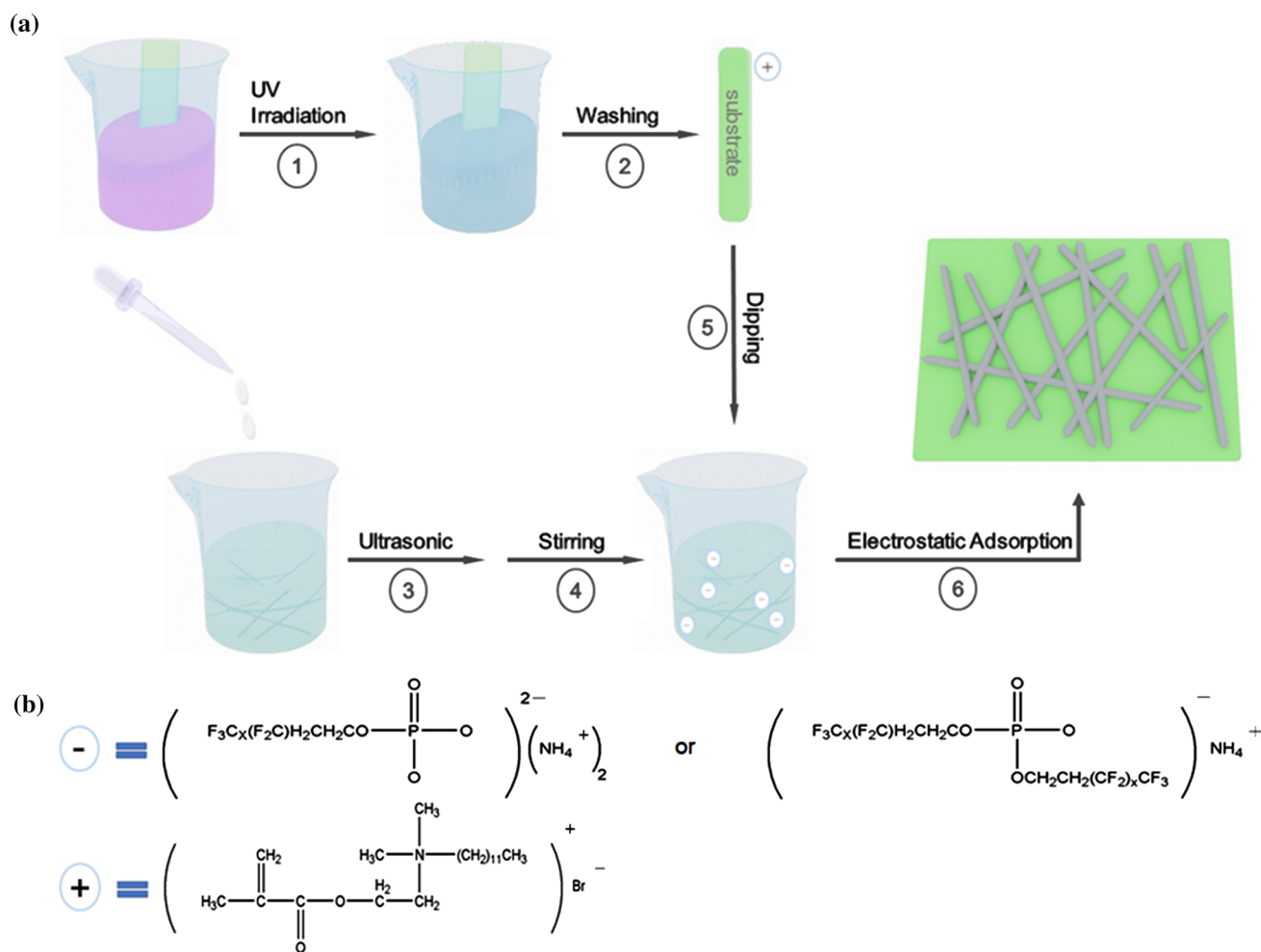


**Figure 1** a Schematic of preparation process of AgNW network on PET film by electrostatic adsorption self-assembly method. b Molecular structures of two typical surfactants, Zonyl® FSP and DMAEMA-R<sub>12</sub>Br.

respectively. These emerging functional groups clearly demonstrated that the modified PET film contained DMAEMA. Meanwhile, the O 1s spectrum also produced a new peak at the 532.3 eV (C–O–C). When the photoreactive group (C=O) of the PET substrate and the carbon–carbon double bond (C=C) of DMAEMA were cleft by UV irradiation, the opened chemical bonds could recombine into a new group of C–O–C. The presence of the C–O–C group testified that the DMAEMA had been successfully grafted onto the PET film. Moreover, there were also new peaks appearing in the N 1s and Br 3d spectra when the quaternary amine monomers were grafted onto the PET film. In particular, the single peak of quaternary amine at 402.3 eV in the N 1s spectrum suggested that the quaternization of DMAEMA was extremely complete.

When a virgin PET film and a modified PET film were immersed in  $5 \times 10^{-4}$  M aqueous Acid Orange 7 solution at 50 °C for 30 min, it was noted that the modified PET film could be dyed with the Acid Orange 7 and the virgin PET film could not be stained, as shown in Fig. 3. Since the Acid Orange 7 can be negatively charged in solution, it is often used to detect cationic surfactants by spectrophotometric [31]. When the Acid Orange 7 was adsorbed on the modified PET film, it demonstrated that the modified PET film had been successfully positively charged in solution.

The as-prepared AgNWs were carefully cleaned and then redispersed in aqueous solution with an anionic surface-active agent. To prove the anionic surfactant successfully adsorbed on AgNWs, XPS and FTIR spectra are used as shown in Fig. 4. In Fig. 4a, the C 1s core level spectrum clearly showed

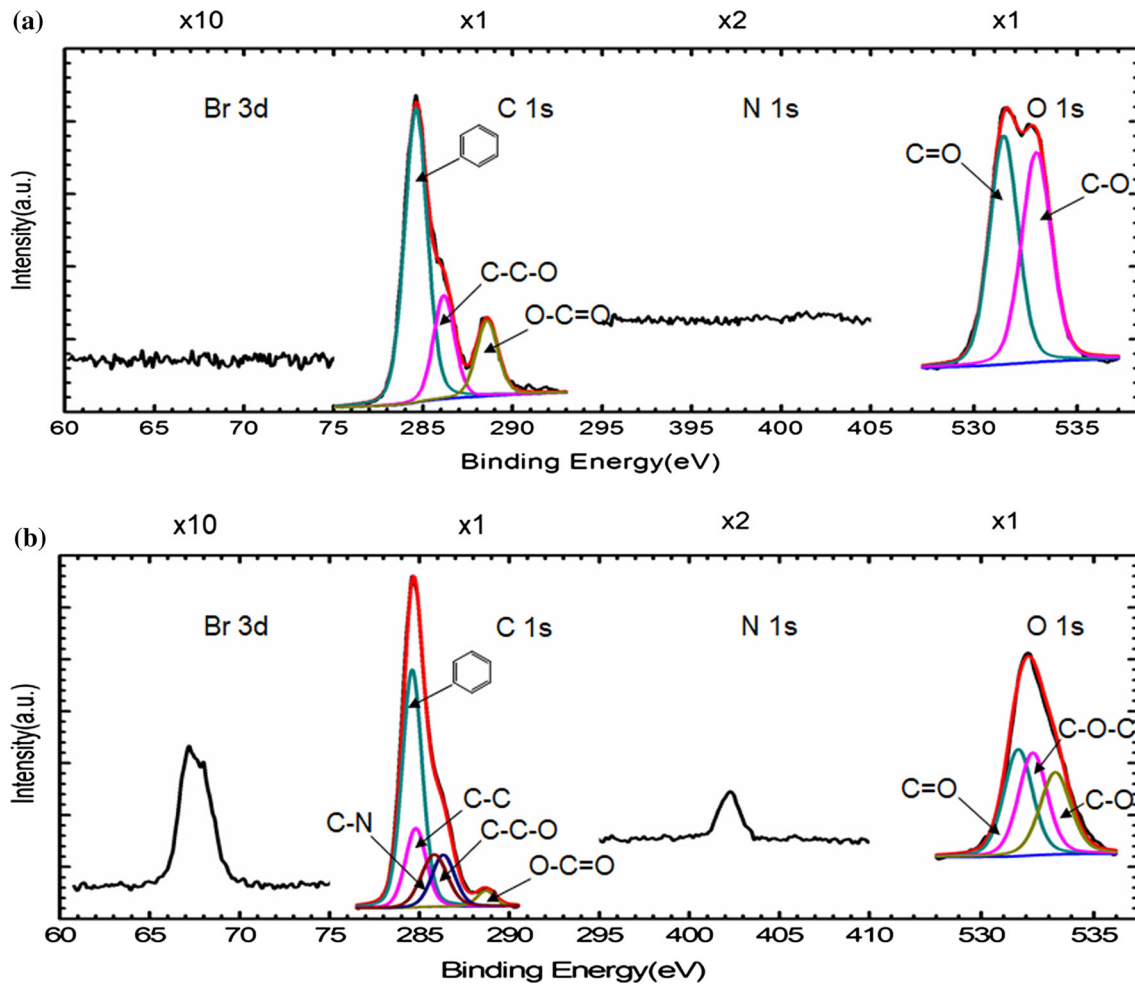


**Figure 2** XPS spectra of the PET film: **a** virgin film, **b** modified film (graft polymerization of DMAEMA-R<sub>12</sub>Br onto PET film).

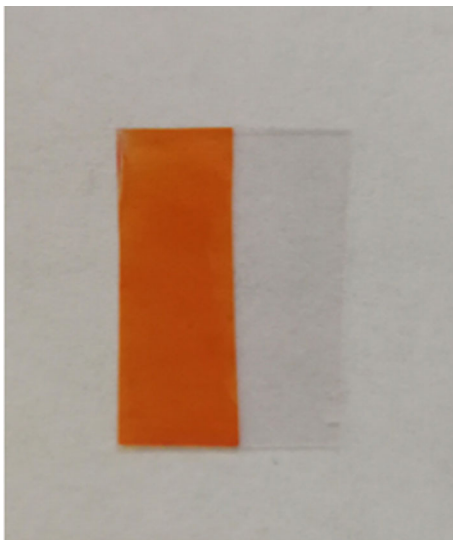


**Figure 3** Photograph of virgin and modified PET films after dipping into Acid Orange 7 solution.

that pristine AgNWs possessed four types of carbon functional groups, i.e., C–N, C–C, C–H, N–C=O. This result demonstrated the pristine AgNWs containing PVP. It was noted that there was no obvious peak in the P 2*p* spectrum of the pristine AgNWs. For redispersed AgNWs, the C 1*s* spectrum contained five main types of carbon functional groups, which were clearly recognizable as C–C (284.6 eV), C–O (285.6 eV), CH<sub>2</sub>–CF<sub>2</sub> (289.5 eV), CF<sub>2</sub>–CF<sub>2</sub> (290.2 eV) and CF<sub>3</sub> (292.2 eV) by binding energy. In this study, the anion surfactant was required to adsorb on AgNWs. According to the XPS C 1*s* spectrum, these new peaks (CH<sub>2</sub>–CF<sub>2</sub>, CF<sub>2</sub>–CF<sub>2</sub> and CF<sub>3</sub>) indicated the redispersed AgNWs contained the anionic surface-active agent (Zonyl® FSP). In addition, the new peak appearing in the P 2*p* spectrum was also consistent with the result, as shown in Fig. 4b. Figure 4c shows FTIR spectra of the pristine AgNWs and the redispersed AgNWs. Compared with the spectrum of the

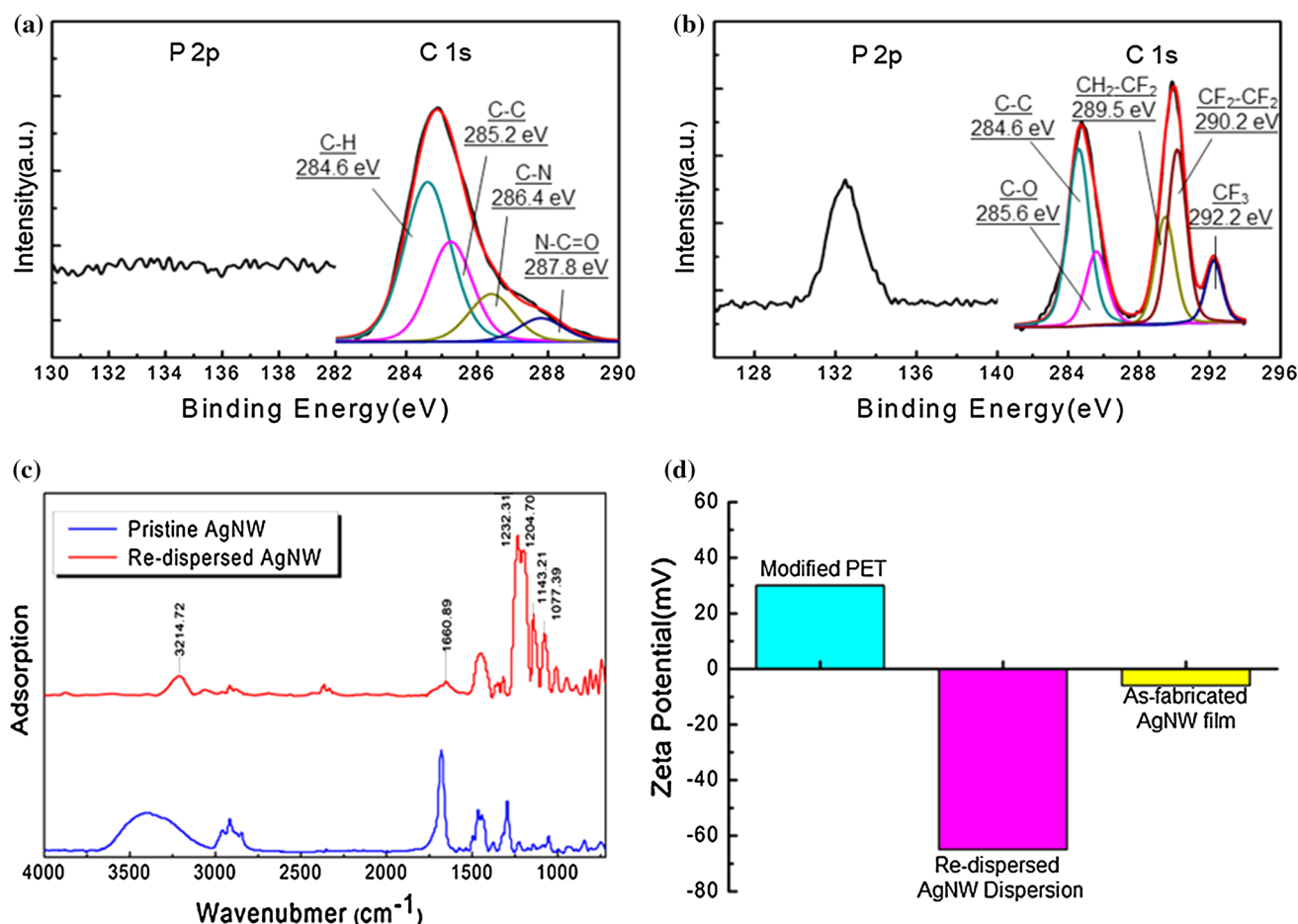


**Figure 4** XPS spectra of **a** pristine AgNWs, and **b** re-dispersed AgNWs. **c** FTIR spectra of re-dispersed AgNWs, compared with pristine AgNWs. **d** Zeta potentials of modified PET, re-dispersed AgNW dispersion and as-fabricated AgNW film.

pristine AgNWs, the weak peak at  $1660.89\text{ cm}^{-1}$  was in correspondence to amide I band (mainly C=O stretching), which indicated that the re-dispersed AgNWs still contained trace PVP. Moreover, in the spectrum of re-dispersed AgNWs, the strong peaks at  $1204.70$  and  $1232.31\text{ cm}^{-1}$  belonged to CF<sub>2</sub> absorption band. The characteristic peaks at  $1143.21$  and  $1077.39\text{ cm}^{-1}$  were attributed to P=O stretching and P-O-C bending, respectively. Meanwhile  $3214.72\text{ cm}^{-1}$  represented the existence of ammonium group. These results supported that the Zonyl<sup>®</sup> FSP was successfully adsorbed on AgNWs.

In this study, the prerequisite for obtaining high reliable conductive films was strong electrostatic adsorption between substrates and AgNWs. The most efficient way to determine this was by zeta potential measurement. As shown in Fig. 4d, when the pH was 7.0 and the temperature was  $25\text{ }^{\circ}\text{C}$ , the zeta potential of a modified PET film was ca.

+ 30 mV because of graft polymerization of DMAEMA-R<sub>12</sub>Br onto PET film. Under the same condition, the zeta potential of the re-dispersed AgNW dispersion was ca. - 63 mV due to the anionic surfactant successfully adsorbed on AgNWs. After the modified PET film was dipped into the re-dispersed AgNW dispersion, the zeta potential of the as-fabricated conductive film was ca. - 6 mV, which demonstrated that the AgNWs were deposited on the PET substrate due to strong electrostatic adsorption.

Figure 5 shows morphologies of AgNW networks adsorbing on PET substrates. After the modified PET film was dipped into AgNW dispersion with the concentration of  $1.5\text{ mg mL}^{-1}$  for 20 min, the obtained AgNW networks had a sheet resistance of  $50\text{ }\Omega\text{ sq}^{-1}$  and an optical transmittance of 73%, as shown in Fig. 5a. With reducing the concentration of dispersion solution to  $0.75\text{ mg mL}^{-1}$ , the density of

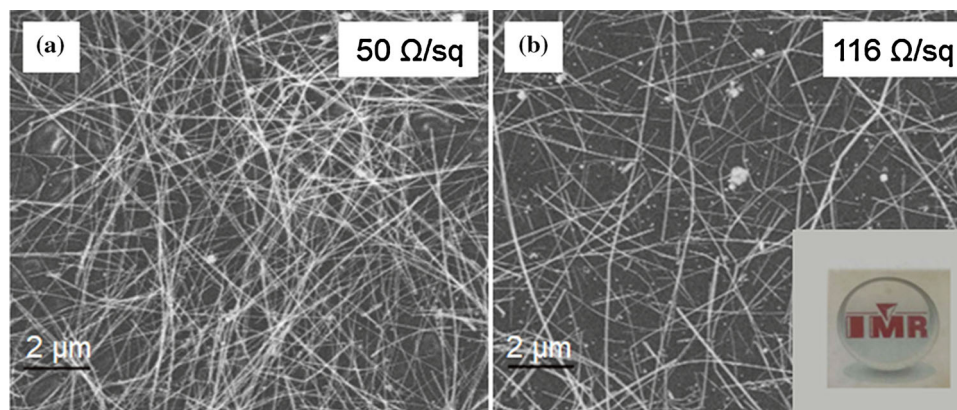
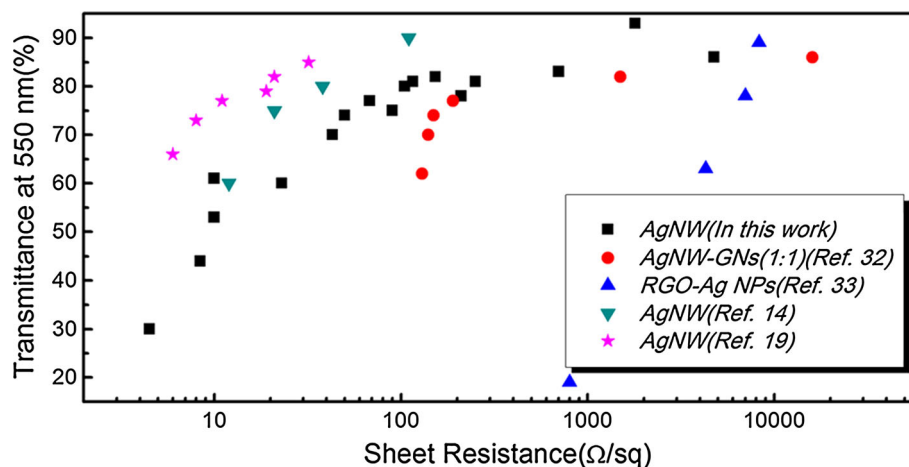


**Figure 5** SEM images of AgNW networks on PET substrates by electrostatic adsorption process. The different densities of the AgNW networks lead to different sheet resistance: **a**  $50 \Omega \text{ sq}^{-1}$ ,

and **b**  $116 \Omega \text{ sq}^{-1}$ . Inset was a photograph of the as-fabricated nanowire network on a  $2 \text{ cm} \times 2 \text{ cm}$  PET substrate.

**Figure 6** Optoelectrical performance comparison between AgNW films in this work and reported conductive films.



the formed AgNW networks was obviously decreased, as shown in Fig. 5b. The sheet resistance and optical transmittance were measured to be  $116 \Omega \text{ sq}^{-1}$  and 81%, respectively. It revealed that the density of AgNW networks could be effectively controlled by adjusting the concentration of the dispersion solution. The optimal concentration of AgNW dispersion should be  $0.5\text{--}3 \text{ mg mL}^{-1}$ . In addition, the SEM images also revealed that the AgNW network by this electrostatic adsorption process was rather uniform over the entire PET substrate. The inset was a photograph of the as-fabricated nanowire network on a  $2 \text{ cm} \times 2 \text{ cm}$  PET substrate. The pattern in the background could be clearly seen through this film, indicating that the film was highly transparent. On the other hand, it was noted that the type and quantity of dispersant had a serious influence on the sheet resistance of the

prepared AgNW films by electrostatic adsorption process. To obtain high-quality conductive films, the weight ratio of the added anionic dispersant and AgNWs should be controlled to be about 1:(10–30) in the AgNW dispersion.

The comparison of optoelectrical property between the present work and the previous reports is plotted as shown in Fig. 6. The fabricated AgNW—graphene nanosheets (GNs) (1:1) hybrid conductive film using an electrostatic adsorption process had an optical transmittance 82% and a sheet resistance of  $1500 \Omega \text{ sq}^{-1}$  [32]. The another multilayer conductive film of the reduced graphene oxide/silver nanoparticles (RGO/Ag NPs) had a high sheet resistance of  $7000 \Omega \text{ sq}^{-1}$  at an optical transmittance of 78% [33]. Obviously, in the case of similar optical transmittance, the sheet resistance of the present AgNW film ( $R_s = 116 \Omega \text{ sq}^{-1}$  with  $T = 81\%$ ) was far lower than

those of the graphene or graphene–silver hybrid films. The reported AgNW conductive films by Meyer rod coating technique and a dry transfer technique shown in Fig. 6 had relatively excellent optoelectrical performance [14, 19]. However, the films prepared by these methods might suffer from poor adhesion between AgNW networks and substrates if not the application of binder or mechanical pressure treatment. Besides that, these methods could

only fabricate the AgNW networks on flat substrates with regular shape.

As for the preparation of AgNW dispersion, one of the available strategies to obtain an excellent optoelectrical performance is to synthesize high aspect ratio nanowires [34]. The other approach is to reduce the insulating ligands covered on nanowires because these organic compounds will greatly increase sheet resistance of AgNW films [35]. In practical, it is extremely difficult to remove the organic dispersant on nanowires after forming conductive films. For removing the dispersant on AgNW films, an ion bombardment method was employed in this work, as schematically illustrated in Fig. 7a. When the gas argon was ionized into positively charged argon ions ( $Ar^+$ ) with enough high energy and then bombarded the surface of the sample, the insulating ligands on the surface could be sputtered and break away from the surface. The plot of sheet resistance versus optical transmittance of the as-prepared AgNW films before and after ion bombardment treatment is shown in Fig. 7b. For any a selected sample prepared in AgNW dispersion with different concentration and amounts of dispersant, the sheet resistance was obviously reduced while the optical transmittance was almost unchanged after ion bombardment treatment. For example, the sample with a large amount of dispersant had a high sheet resistance of  $2361 \Omega \text{ sq}^{-1}$ . After ion bombardment, the sheet resistance was decreased to  $45 \Omega \text{ sq}^{-1}$  and the transmittance was still 70%. In comparison, the samples with a small amount of dispersant had a relatively small decrease in sheet resistance after ion bombardment. The results reflected the effectiveness of ion bombardment on removing the dispersant on AgNW films.

Table 1 shows the sheet resistance of the AgNW films after different ion bombardment time. It was noteworthy that the sheet resistance decreased to a lowest value and then began to increase with the

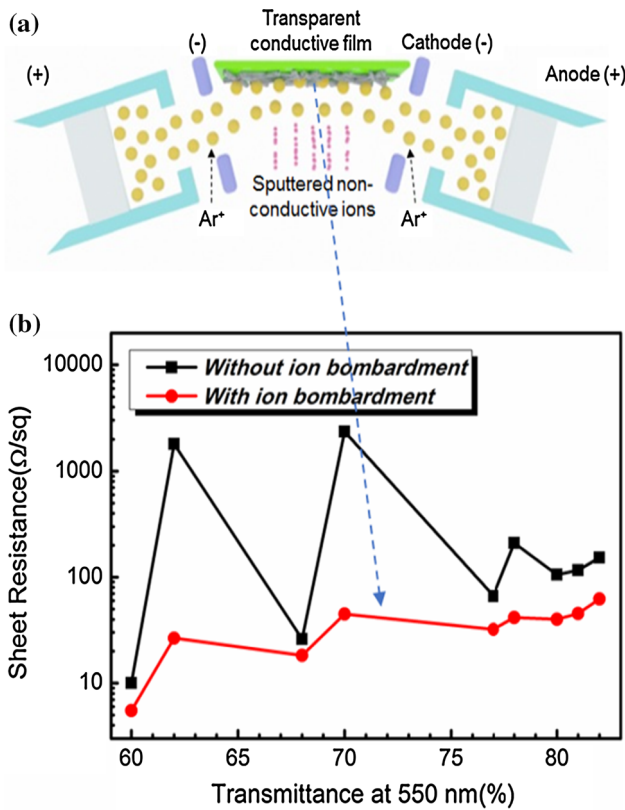


**Figure 7** a Schematic illustration of ion bombardment process to remove dispersant on AgNW films. b Change of sheet resistance versus transmittance at 550 nm for AgNW films after ion bombardment.

**Table 1** Sheet resistance change of the AgNW conductive films for varied ion bombardment treatment time

Sample	Sheet resistance ( $\Omega \text{ sq}^{-1}$ ) with varied ion bombardment time (s)					
	0	60	90	180	240	300
Sample1	23	18.1	15.1	38.8		
Sample2	1800		81.2	48.0	33.1	52.5
Sample3	50	39.1	32.5	55.3		
Sample4	451		85.4	45.2	71.3	



increasing bombardment time. It was thought that the over-long time treatment could damage the silver nanowire network, which would increase the sheet resistance. Additionally, the bombardment time to reach the minimum sheet resistance was different among these samples. The required bombardment time to obtain optimum optoelectrical performance was related to the amount of the dispersant adsorbed on nanowires.

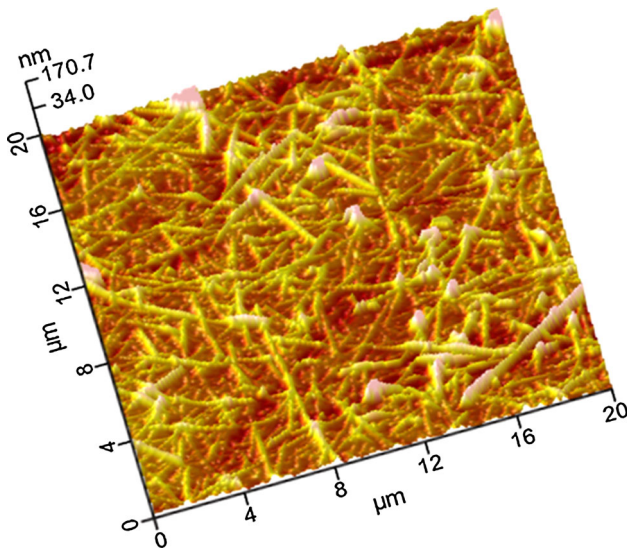


**Figure 8** AFM image of the AgNW film prepared by electrostatic adsorption self-assembly process. The scale range was  $20 \mu\text{m} \times 20 \mu\text{m}$ .

Surface roughness is one of crucial property parameters for the application of TCFs. It was reported that the solution processed AgNW conductive films often exhibited high surface roughness if not a post-treatment process [36]. In contrast to the common spinning coating or Meyer rod coating process [14, 37], this self-assemble process was capable of forming monolayer films and building a nearly flat AgNW network. Therefore, the conductive film prepared by the present method could possess a relatively low surface roughness. As shown in Fig. 8, the surface roughness value was measured to be 25.2 nm. Such a low surface roughness could allow for strong bonding force and be well compatible with high-efficiency optoelectronic devices.

The reliability of the as-fabricated flexible conductive films was evaluated by a cyclic bending test on a custom-designed apparatus (inset in Fig. 9b). When a cyclic bending loading with 10 mm bending radius was carried out on the as-prepared sample, the change of the normalized resistance ( $R/R_0$ ) was monitored in real time, as shown in Fig. 9a. It was shown that the change of  $R/R_0$  was almost unnoticeable after 10000 cycles. Also, the bending radius had hardly effect on the resistance of the conductive films, as shown in Fig. 9b. After the high-cycle bending fatigue, the AgNW network was not detected to be damaged or detached from the substrate. Even without the usage of binder, the cohesion between AgNW networks and PET substrates was quite reliable due to the strong electrostatic adsorp-

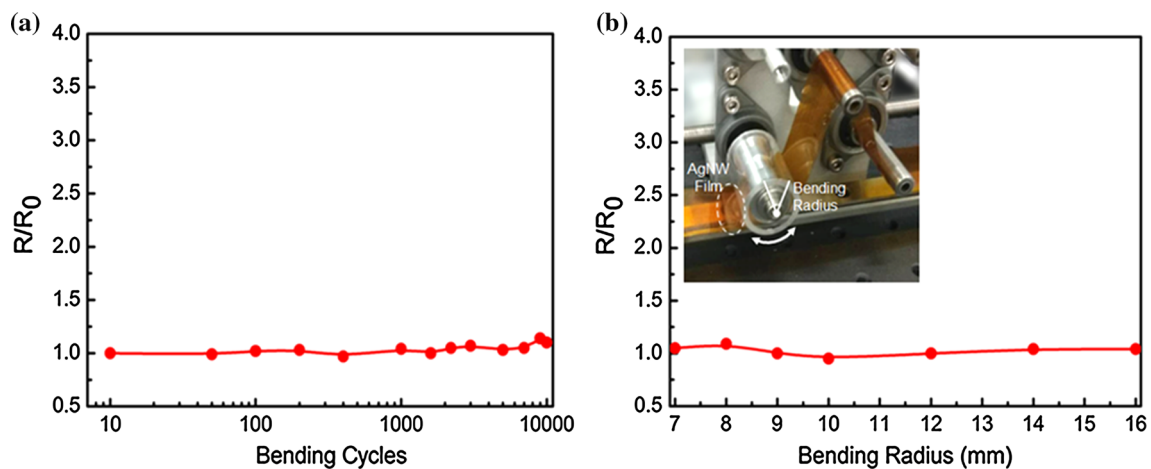


**Figure 9** **a** The  $R/R_0$  change with the bending cycles at the bending radius of 10 mm. **b** The  $R/R_0$  values after 1000 bending cycles with various bending radius. Inset showed a custom-designed bending test apparatus.

tion. This flexible AgNW conductive film prepared by electrostatic adsorption method showed a potential application in the future flexible devices.

## Conclusions

In this work, a flexible AgNW conductive network on PET substrate was fabricated by an electrostatic adsorption self-assembly process. The electrostatic adsorption self-assembly process was accomplished by immersing the modified PET into the AgNW dispersion with anionic dispersant. Without a post-treatment process, the formed AgNW network on PET substrate could achieve a relatively low sheet resistance of  $116 \Omega \text{ sq}^{-1}$  at  $T = 81\%$ . The sheet resistance of the AgNW films could be further decreased to  $45.3 \Omega \text{ sq}^{-1}$  when the insulating ligands on AgNWs were removed by an ion bombardment method. In addition, the test results showed that the as-prepared flexible AgNW films had low surface roughness and high reliability. Since this method is easily operated and independent on the shape and size of the substrate, it is expected to broaden the application range of AgNW conductive films in optoelectronic devices.

## Acknowledgements

This study was financially supported by the National Natural Science Foundation of China (NSFC), under the Grant No. 51471180, and Science and Technology Program of Shenyang, under the Grant No. F16-205-1-18.

## Compliance with ethical standards

**Conflict of interest** The authors declare that they have no conflict of interest.

## References

- Granqvist CG (2007) Transparent conductors as solar energy materials: a panoramic review. *Sol Energy Mater Sol Cells* 91:1529–1598
- Gaynor W, Burkhard GF, McGehee MD, Peumans P (2011) Smooth nanowire/polymer composite transparent electrodes. *Adv Mater* 23:2905–2910
- Du JH, Pei SF, Ma LP, Cheng HM (2014) Carbon nanotube- and graphene-based transparent conductive films for optoelectronic devices. *Adv Mater* 26:1958–1991
- De Arco LG, Zhang Y, Schlenker CW, Ryu KM, Thompson ME, Zhou CW (2010) Continuous, highly flexible, and transparent graphene films by chemical vapor deposition for organic photovoltaics. *ACS Nano* 4:2865–2873
- Lee H, Kim M, Kim I, Lee H (2016) Flexible and stretchable optoelectronic devices using silver nanowires and graphene. *Adv. Mater.* 28:4541–4548
- Kumar A, Zhou CW (2010) The race to replace tin-doped indium oxide: which material will win. *ACS Nano* 4:11–14
- Zhang QC, Tang L, Luo J, Zhang J, Wang XN, Li D, Yao YG, Zhang ZX (2017) Direct growth of nanocrystalline graphene/graphite all carbon transparent electrode for graphene glass and photodetectors. *Carbon* 111:1–7
- Chen ZP, Ren WC, Gao LB, Liu BL, Pei SF, Cheng HM (2011) Three-dimensional flexible and conductive interconnected graphene networks grown by chemical vapor deposition. *Nat Mater* 10:424–428
- Cao Q, Rogers JA (2009) Ultrathin films of single-walled carbon nanotubes for electronics and sensors: a review of fundamental and applied aspects. *Adv Mater* 21:29–53
- Zhang DH, Ryu K, Liu XL, Polikarpov E, Tompson ME, Zhou CW (2006) Transparent, conductive, and flexible carbon nanotube films and their application in organic light-emitting diodes. *Nano Lett* 6:1880–1886
- Zhai HT, Wang RR, Wang X, Cheng Y, Shi LJ, Sun J (2016) Transparent heaters based on highly stable Cu nanowire films. *Nano Res* 9:3924–3936
- Lee JY, Connor ST, Cui Y, Peumans P (2008) Solution-processed metal nanowire mesh transparent electrodes. *Nano Lett* 8:689–692
- Garnett EC, Cai WS, Cha JJ, Mahmood F, Connor ST, Christoforo MG, McGehee MD, Brongersma ML (2012) Self-limited plasmonic welding of silver nanowire junctions. *Nat Mater* 11:241–249
- Hu LB, Kim HS, Lee JY, Peumans P, Cui Y (2010) Scalable coating and properties of transparent, flexible, silver nanowire electrodes. *ACS Nano* 4:2955–2963
- Lee D, Lee H, Ahn Y, Lee Y (2015) High-performance flexible transparent conductive film based on graphene/AgNW/graphene sandwich structure. *Carbon* 81:439–446
- Leem DS, Edwards A, Faist M, Nelson J, Bradley DDC, Mello JCD (2011) Efficient organic solar cells with solution-processed silver nanowire electrodes. *Adv Mater* 23:4371–4375
- Zhan K, Su R, Bai SH, Yu ZH, Cheng N, Wang CL, Xu S, Liu W, Guo SS, Zhao XX (2016) One-pot stirring-free synthesis of silver nanowires with tunable lengths and

- diameters via a  $\text{Fe}^{3+}$  &  $\text{Cl}^-$  co-mediated polyol method and their application as transparent conductive films. *Nanoscale* 8:18121–18133
- [18] Selzer F, Weiß N, Knepe D, Bormann L, Sachse C, Gaponik K, Eychmüller A, Leo K, Müller-Meskamp L (2015) A spray-coating process for highly conductive silver nanowire networks as the transparent top-electrode for small molecule organic photovoltaics. *Nanoscale* 7:2777–2783
- [19] Madaria AR, Kumar A, Ishikawa FN, Zhou CW (2010) Uniform, highly conductive, and patterned transparent films of a percolating silver nanowire network on rigid and flexible substrates using a dry transfer technique. *Nano Res* 3:564–573
- [20] Decher G, Hong JD (1991) Buildup of ultrathin multilayer films by a self-assembly process: 1. Consecutive adsorption of anionic and cationic bipolar amphiphiles on charged surfaces. *Macromol Chem Macromol Symp* 46:321–327
- [21] Decher G (1997) Fuzzy nanoassemblies: toward layered polymeric multicomposites. *Science* 277:1232–1237
- [22] Chen W, McCarthy TJ (1997) Layer-by-layer deposition: a tool for polymer surface modification. *Macromolecules* 30:78–86
- [23] Han Y, Sukhishvili S, Du H, Cefaloni J, Smolinski B (2008) Layer-by-layer self-assembly of oppositely charged nanoparticles on silica microspheres for trace analysis of aqueous solutions using surface-enhanced Raman scattering. *J Nanosci Nanotechnol* 8:5791–5800
- [24] Lee H, Han G, Kim M, Ahn HS, Lee H (2015) High mechanical and tribological stability of an elastic ultrathin overcoating layer for flexible silver nanowire films. *Adv Mater* 27:2252–2259
- [25] Yu B, Liu XM, Cong HL, Wang ZH, Lian YC, Tang JG (2014) Fabrication of stable ultrathin transparent conductive carbon nanotube micropatterns using layer-by-layer self-assembly. *Fuller Nanotub Carbon Nanostructures* 23:320–325
- [26] Sannicolo T, Munoz-Rojas D, Nguyen ND, Moreau S, Celle C, Simonato JP, Brechet Y, Bellet D (2016) Direct imaging of the onset of electrical conduction in silver nanowire networks by infrared thermography: evidence of geometrical quantized percolation. *Nano Lett* 16:7046–7053
- [27] Park JH, Hwang GT, Kim S, Seo J, Park HJ, Yu K, Kim TS, Lee KJ (2017) Flash-induced self-limited plasmonic welding of silver nanowire network for transparent flexible energy harvester. *Adv Mater* 29:1603473
- [28] Kholmanov IN, Stoller MD, Edgeworth J, Lee WH, Li H, Lee J, Barnhart C, Potts JR, Piner R, Akinwande D (2012) Nanostructured hybrid transparent conductive films with antibacterial properties. *ACS Nano* 6:5157–5163
- [29] Uchida E, Ikada Y (1996) Introduction of quaternary amines onto a film surface by graft polymerization. *J Appl Polym Sci* 61:1365–1373
- [30] Clark DT, Thomas HR (1978) Applications of ESCA to polymer chemistry. 17. Systematic investigation of the core levels of simple homopolymers. *J Polym Sci Polym Chem Ed* 16:791–820
- [31] Yamamoto K, Motomizu S (1991) Spectrophotometric method for the determination of ionic surfactants by flow-injection analysis with acidic dyes. *Anal Chim Acta* 246:333–339
- [32] Tien HW, Hsiao ST, Liao WH, Yu YH, Lin FC, Wang YS, Li SM, Ma CCM (2013) Using self-assembly to prepare a graphene-silver nanowire hybrid film that is transparent and electrically conductive. *Carbon* 58:198–207
- [33] Zhou YZ, Yang J, Cheng XN, Zhao N, Sun HB, Li D (2013) Transparent and conductive reduced graphene oxide/silver nanoparticles multilayer film obtained by electrical self-assembly process with graphene oxide sheets and silver colloid. *RSC Adv* 3:3391–3398
- [34] Chen YH, Rathmell AR, Charbonneau P, Li ZY, Wiley BJ (2012) The effect of nanowire length and diameter on the properties of transparent, conducting nanowire films. *Nanoscale* 4:1996–2004
- [35] Lee J, Lee I, Kim TS, Lee JY (2013) Efficient welding of silver nanowire networks without post-processing. *Small* 9:2887–2894
- [36] Guo CF, Ren ZF (2015) Flexible transparent conductors based on metal nanowire networks. *Mater. Today* 18:143–154
- [37] Jiang YQ, Xi J, Wu ZX, Dong H, Zhao ZX, Jiao B, Hou X (2015) Highly transparent, conductive, flexible resin films embedded with silver nanowires. *Langmuir* 31:4950–4957